

# Up-regulation of autophagy by low concentration of salicylic acid delays methyl jasmonate-induced leaf senescence

**Runzhu Yin**

South China Normal University

**Xueyan Liu**

Jinan University

**Jingfang Yu**

South China Normal University

**Yingbin Ji**

South China Normal University

**Jian Liu**

Fujian Agriculture and Forestry University

**Lixin Cheng**

Jinan University

**Jun Zhou** (✉ [zhoujun@scnu.edu.cn](mailto:zhoujun@scnu.edu.cn))

South China Normal University <https://orcid.org/0000-0001-9655-6588>

---

## Research article

**Keywords:** autophagy, gene modules, jasmonic acid, leaf senescence, RNA-Seq, salicylic acid

**Posted Date:** December 13th, 2019

**DOI:** <https://doi.org/10.21203/rs.2.18798/v1>

**License:** © ⓘ This work is licensed under a Creative Commons Attribution 4.0 International License.

[Read Full License](#)

---

**Version of Record:** A version of this preprint was published at Scientific Reports on July 10th, 2020. See the published version at <https://doi.org/10.1038/s41598-020-68484-3>.

1 **Up-regulation of autophagy by low concentration of salicylic acid delays**  
2 **methyl jasmonate-induced leaf senescence**

3 Runzhu Yin<sup>1#</sup>, Xueyan Liu<sup>2#</sup>, Jingfang Yu<sup>1</sup>, Yingbin Ji<sup>1,3</sup>, Jian Liu<sup>4</sup>, Lixin Cheng<sup>2\*</sup>, Jun  
4 Zhou<sup>1\*</sup>

5 1 MOE Key Laboratory of Laser Life Science & Guangdong Provincial Key Laboratory of  
6 Laser Life Science, College of Biophotonics, South China Normal University, Guangzhou  
7 510631, China

8 2 Department of Critical Care Medicine, Shenzhen People's Hospital, The Second Clinical  
9 Medicine College of Jinan University, Shenzhen 518020, China

10 3 Luoyang Tmaxtree Biotechnology Co., Ltd, Luoyang 471023, China

11 4 Fujian Provincial Key Laboratory of Plant Functional Biology, College of Life Sciences,  
12 Fujian Agriculture and Forestry University, Fuzhou 350002, China

13 \*Correspondence authors: Jun Zhou, [zhoujun@scnu.edu.cn](mailto:zhoujun@scnu.edu.cn); Lixin Cheng,  
14 [easonlcheng@gmail.com](mailto:easonlcheng@gmail.com);

15 # These authors contributed equally to this work.

16 **Running title:** Role of autophagy in LCSA-delayed leaf senescence.

17

18 **ABSTRACT**

19 Crosstalk between salicylic acid (SA) and jasmonic acid (JA) signaling plays an important  
20 role in molecular regulation of plant senescence. Our previous works found that SA could  
21 delay methyl jasmonate (MeJA)-induced leaf senescence in a concentration-dependent  
22 manner. Here, the effect of low concentration of SA (LCSA) application on MeJA-induced  
23 leaf senescence was further assessed. High-throughput sequencing (RNA-Seq) results  
24 showed that LCSA did not have dominant effects on the genetic regulatory pathways of  
25 basal metabolism like nitrogen metabolism, photosynthesis and glycolysis. The  
26 ClusterONE was applied to identify discrete gene modules based on protein-protein  
27 interaction (PPI) network. Interestingly, an autophagy-related (ATG) module was identified  
28 in the differentially expressed genes (DEGs) that exclusively induced by MeJA together  
29 with LCSA. RT-qPCR confirmed that the expression of most of the determined ATG genes  
30 were upregulated by LCSA. Remarkably, in contrast to wild type (Col-0), LCSA cannot  
31 alleviate the leaf yellowing phenotype in autophagy defective mutants (*atg5-1* and *atg7-2*)  
32 upon MeJA treatment. Confocal results showed that LCSA increased the number of  
33 autophagic bodies accumulated in the vacuole during MeJA-induced leaf senescence.  
34 Collectively, our work revealed up-regulation of autophagy by LCSA as a key regulator to  
35 alleviate MeJA-induced leaf senescence.

36 **Key Words:** autophagy; gene modules; jasmonic acid; leaf senescence; RNA-Seq;  
37 salicylic acid

38

## 39 INTRODUCTION

40 Senescence in green plants is a complex and orderly regulated process that is crucial for  
41 transiting from nutrient assimilation to nutrient remobilization (Masclaux et al., 2000;  
42 Quirino et al., 2000; Lim et al., 2003; Yoshida, 2003; Schippers, 2015). During senescence,  
43 the most visible characteristic is leaf yellowing, which is the consequence of a succession  
44 of changes in cellular physiology including chlorophyll degradation and photosynthetic  
45 activity reduction (Lim et al., 2003; Yoshida, 2003). Chloroplast as an early senescence  
46 signaling response organelle, its dismantling plays an important role in the major nitrogen  
47 source recycling and remobilization (Avila-Ospina et al., 2014). The progression of leaf  
48 senescence can be prematurely induced by multiple environmental and endogenous  
49 factors, such as temperature, light, humidity and phytohormones (Lim et al., 2007).  
50 Hormone signaling pathways play roles at all the stages of leaf senescence, including the  
51 initiation, progression, and the terminal phases of senescence (Lim et al., 2007). Recent  
52 progresses show that senescence can be coordinately regulated by several  
53 phytohormones like cytokinins, ethylene, abscisic acid, salicylic acid (SA), and jasmonic  
54 acid (JA) (Gan and Amasino, 1995; van der Graaff et al., 2006; Hung and Kao, 2004; He  
55 et al., 2002; Morris et al., 2000). However, the detailed molecular mechanisms for these  
56 phytohormone signals in plant senescence remain poorly understood.

57 JA has been known as a key plant hormone for promoting senescence, based on the  
58 findings that exogenously applied methyl jasmonate (MeJA, methyl ester of JA) leads to a  
59 rapid loss of chlorophyll content and accompany with reduction of photochemical efficiency  
60 (Yue et al., 2012; Ji et al., 2016). Studies with JA-insensitive mutant *coronatine insensitive*  
61 *1 (coi1)* that exhibited defective senescence response to MeJA treatment (He et al., 2002),  
62 supporting the notion that JA signaling pathway is crucial for leaf senescence. Some other  
63 evidences indicate that SA is also involved in plant senescence (Morris et al., 2000; Chai  
64 et al., 2014). The concentration of endogenous SA increases to upregulate several  
65 senescence-associated genes during leaf senescence (Morris et al., 2000; Yoshimoto et  
66 al., 2009). However, such genetic regulatory mechanisms are abolished in plants defective  
67 in the SA signaling or biosynthetic pathway (*npr1* and *pad4* mutants, and *NahG* transgenic  
68 plants) (Morris et al., 2000). Crosstalk between MeJA and SA has been broadly  
69 documented in plant defense response, which commonly manifests as a reciprocal  
70 antagonism pattern (Thaler et al., 2012). Evidence suggests that antagonistic interactions  
71 between SA and MeJA modulate the expression of a senescence-specific transcription  
72 factor WRKY53, showing induced by SA, but repressed by MeJA (Miao and Zentgraf,

73 2007). Overall, mechanisms determining the specificity and coordination between SA and  
74 JA still need to be further explored.

75 Most of phytohormones have both stimulatory and inhibitory effects on the growth and  
76 metabolism of higher plants in a dose dependent manner. It seems that SA functions in the  
77 same way on the physiological and biochemical processes of plants (Ji et al., 2016;  
78 Pasternak et al., 2019). Low-concentration SA (hereafter as LCSA) at below 50 micromole  
79 ( $\mu\text{M}$ ) promotes adventitious roots and altered architecture of the root apical meristem,  
80 whereas high-concentration SA (greater than 50  $\mu\text{M}$ ) inhibits root growth (Pasternak et al.,  
81 2019). Interestingly, we previously demonstrated that MeJA-induced leaf senescence  
82 could be delayed by LCSA (1-50  $\mu\text{M}$ ), but accelerated when the concentration higher than  
83 100  $\mu\text{M}$  (Ji et al., 2016). Our other related works have verified such high dose of SA greatly  
84 activates NPR1 (nonexpressor of pathogenesis-related genes 1) translocation into nucleus,  
85 thereby promoting leaf senescence (Chai et al., 2014). Based on the dose dependent effect  
86 of SA, Pasternak et al. (2019) proposes that at low levels it acts as a developmental  
87 regulator and at high levels it acts as a stress hormone.

88 Autophagy is associated with plant senescence as defective mutants display early and  
89 strong yellowing leaf symptoms (Hanaoka et al., 2002; Xiong et al., 2005; Avila-Ospina et  
90 al., 2014; Li et al., 2014). Autophagy negatively regulates cell death by controlling NPR1-  
91 dependent SA signaling during senescence in Arabidopsis (Yoshimoto et al., 2009). The  
92 senescence process always accompanies with the equilibrium between oxidative and  
93 antioxidative capacities of the plant, which creates a characteristic oxidative environment  
94 resulting in the production of reactive oxygen species (ROS) and more toxic derivatives  
95 (Bhattacharjee, 2005). Moreover, autophagy is involved in the degradation of oxidized  
96 proteins under oxidative stress conditions in Arabidopsis (Xiong et al., 2007). Actually, there  
97 is a complicated interplay between ROS and autophagy, i.e., ROS can induce autophagy  
98 while autophagy be able to reduce ROS production (Signorelli et al., 2009). Our previous  
99 studies showed that LCSA application delays senescence by enhancing the activities of  
100 antioxidant enzymes and restricting reactive oxygen species (ROS) accumulation in MeJA-  
101 treated leaves (Ji et al., 2016). However, it is still unclear whether autophagy pathway is  
102 implicated in the LCSA-alleviated leaf senescence.

103 Here, the interactions between SA and MeJA in plant senescence were further  
104 investigated. By applying transcriptome and interaction network analysis, we identified  
105 autophagy-related (ATG) gene module. In contrast to wild type (Col-0), LCSA cannot  
106 alleviate the leaf yellowing phenotype in autophagy defective mutants upon MeJA

107 treatment. Further results revealed that LCSA increased the number of autophagic bodies  
108 during MeJA-induced leaf senescence. Collectively, our work provides new insight that up-  
109 regulation of autophagy by LCSA is a key regulator to alleviate MeJA-induced leaf  
110 senescence.

## 111 **MATERIALS AND METHODS**

### 112 **Plant materials and chemical treatments**

113 Arabidopsis plants of wild-type (WT, Col-0), *atg5-1* (SAIL\_129\_B07), *atg7-2* (GK-655B06)  
114 and eYFP-ATG8e (Zhuang et al., 2013) were grown in a greenhouse at 22 °C with 16 h  
115 light photoperiod (120  $\mu\text{mol quanta}^{-2} \text{ m}^{-2}$ ). Phytohormones treatment was performed as  
116 described by Ji et al (2016). Briefly, the 3rd and 4th rosette leaves from four weeks of plants  
117 were detached and incubated in 3 mM MES buffer (pH 5.8) containing 50  $\mu\text{M}$  methyl  
118 jasmonate (MeJA) and/or 10  $\mu\text{M}$  salicylic acid (SA). MeJA was prepared from a 50 mM  
119 stock solution in ethanol. Solutions without MeJA were supplemented with equal amounts  
120 of ethanol. Concanamycin A (ConcA) was prepared as a 1 mM stock solution in DMSO and  
121 used at final concentration 1  $\mu\text{M}$ .

### 122 **Photochemical efficiency and chlorophyll content measurements**

123 The photochemical efficiency was measured with an Imaging-PAM Chlorophyll  
124 Fluorometer (PAM-MINI, Walz, Germany) followed the procedure described previously  
125 (Zhou et al., 2015). After dark-adapted for 1 h, parameters  $F_o$  (minimum fluorescence with  
126 PSII reaction centers fully open) and  $F_m$  (maximum fluorescence after dark adaptation)  
127 were acquired with a 0.8-s saturating pulse (4,000  $\mu\text{mol photons m}^{-2} \text{ s}^{-1}$ ). The value of  
128  $F_v/F_m$  was calculated by the formulas  $(F_m - F_o)/F_m$ . Total Chlorophyll was determined as  
129 reported by Coombs et al. (1987). Chlorophyll was extracted by immersion in 90% ethanol  
130 at 65 °C for 2 h. The absorbance at 664 nm and 647 nm were determined with a Lambda  
131 35 UV/VIS Spectrometer (Perkin-Elmer) (Zeng et al., 2016). The concentration per fresh  
132 weight of leaf tissue was calculated according to the formula: micromoles of chlorophyll  
133 per milliliter per gram fresh weight =  $7.93(A_{664}) + 19.53(A_{647})$ . The percentages of  $F_v/F_m$   
134 and chlorophyll content are calculated relative to the initial levels of samples before  
135 treatment (time zero).

### 136 **RNA-Seq analysis**

137 Detached 3rd and 4th rosette leaves from 4-week old plants were immersed in 3 mM MES  
138 buffer (pH 5.8) containing 10  $\mu\text{M}$  SA, 50  $\mu\text{M}$  MeJA, and MeJA together with SA for 24 h.

139 Total RNA for RNA-Seq was extracted from leaves using a Hipure plant RNA kit (Magen,  
140 China). Purified RNA was analyzed either using a ND-1000 Nanodrop (Thermo Fisher,  
141 USA), or by agarose gel electrophoresis to determine the RNA quantity. Those RNA  
142 samples with no smear seen on agarose gels, a 260/280 ratio above 2.0, and RNA integrity  
143 number greater than 8.0 were used. For RNA-Seq analysis, we mixed three replication  
144 samples for each treatment into one, and total RNA samples were then sent to RiboBio  
145 Co., Ltd (Guangzhou, China) for sequencing. The NEBNext Poly(A) mRNA Magnetic  
146 Isolation Module (NEB, USA) was used for mRNA purification. The Ultra II RNA Library  
147 Prep Kit for Illumina was used for RNA library construction. The libraries were sequenced  
148 as 50-bp single end reads using Illumina HiSeq2500 according to the manufacturer's  
149 instructions.

### 150 **Differential Expression Analysis**

151 Raw read count of each gene was generated using HTSeq with union-count mode (Love  
152 et al., 2014). After normalization by Reads Per Kilobase per Million mapped reads (rpkm),  
153 normalized read count table was used for determining differentially expressed genes  
154 (DEGs) (Anders and Huber, 2010; Cheng et al., 2016a, 2016b), which were defined as  
155 those with 2-fold changes. Fold change was calculated using  $\log_2$  (normalized read  
156 count+1). An R package *clusterprofiler* was used to perform the functional category  
157 analysis to detect the significantly enriched Gene Ontology (GO) terms (Cheng and Leung,  
158 2018a, and 2018b). Significantly enriched GO terms were selected by a threshold of  $p \leq$   
159 0.05. Protein-protein interaction (PPI) data was obtained from the STRING database (v.10,  
160 <http://string-db.org>) (Szklarczyk et al., 2014). To construct a high-confidence network, only  
161 the PPIs with confidence scores larger than 0.7 were considered in this work. ClusterONE  
162 was adopted for the identification of protein clusters or functional modules using default  
163 parameters as described previously (Cheng et al., 2017; Cheng et al., 2019). The protein  
164 modules including five or more than five members and having connection density over 0.5  
165 are defined as modules.

### 166 **RT-qPCR**

167 Total RNA was isolated using Eastep Super RNA Kit (Promega, Shanghai, China) and  
168 genomic DNA was removed using DNase I. 1  $\mu\text{g}$  of RNA was used to make cDNA with the  
169 GoScript™ Reverse Transcription System (Promega, Shanghai, China). For qPCR 10  $\mu\text{L}$   
170 of Green-2-Go 2X qPCR-S Mastermix (Sangon, Shanghai, China) and 1  $\mu\text{L}$  of cDNA (100  
171 ng/ $\mu\text{L}$ ) for a total of 20  $\mu\text{L}$  was used in each well. Real-time PCR was done on a CFX

172 Connect Real-Time System (BioRad) at 95 °C for 2 mins, and 45 cycles of 95 °C for 15 s,  
173 55 °C for 30s, and 72 °C for 30s followed by a melting curve analysis. For each sample 3  
174 biological reps were used and repeated 3 times for technical replication. qPCR was  
175 analyzed using the  $\Delta\Delta C_t$  method. Primers for qPCR were showed in Table S2. Statistical  
176 significance was determined using Duncan's multiple range test.

### 177 **Confocal microscopy**

178 Detached 3rd and 4th rosette leaves were immersed in 3 mM MES buffer (pH 5.8)  
179 containing 50  $\mu$ M MeJA and/or 10  $\mu$ M SA for 24 h. ConCA (1  $\mu$ M) was added at 6 h before  
180 confocal imaging. Confocal images were captured with 63x (numerical aperture [NA], 1.4)  
181 objective using an LSM 880 microscope (Zeiss). For quantification of autophagic puncta,  
182 randomly selected 15 to 20 images for each three independent experiments were  
183 quantified with ImageJ. All images were collected with the same settings determined prior  
184 to the experiment to yield nonsaturating conditions.

## 185 **RESULTS**

### 186 **LCSA delays MeJA-induced leaf senescence**

187 Our previous results indicated that SA delays MeJA-induced leaf senescence in a  
188 concentration-dependent manner, showing accelerated by high SA concentrations (greater  
189 than 100  $\mu$ M) but attenuated by low SA concentrations (1-50  $\mu$ M) (Ji et al., 2016). On this  
190 basis, 10  $\mu$ M SA, the most effective concentration according to Ji et al., 2016, was selected  
191 as low working solution to further confirm the effect of LCSA. As shown in Figure 1, in  
192 contrast to control, LCSA did not appear to have a discernible effect on senescence.  
193 Leaves incubated with MeJA (50  $\mu$ M) were greatly turned yellow after 5 days treatment.  
194 However, when MeJA worked together with LCSA (MeJA+LCSA), the leaf yellowing was  
195 alleviated (Figure 1A). Consistent with the visible phenotype, the photochemical efficiency  
196 Fv/Fm and loss of chlorophyll content in the leaves combined treatment with LCSA and  
197 MeJA was less severe relative to that of the leaves treated with MeJA alone (Figure 1B  
198 and 1C). These physiological and biochemical data is consistent with our previous finding  
199 that LCSA provide protection against senescence caused by MeJA.

### 200 **Expression patterns of genes in LCSA-induced delayed leaf senescence**

201 To investigate the genome-wide effect of LCSA on MeJA-induced gene expression  
202 changes, we performed RNA-sequencing experiments. Since gene transcription regulation  
203 occurs prior to visible phenotype, leaves treatment with phytohormones at 1 d were

204 selected according to our previous study (Ji et al., 2016). Totally, 408, 2536 and 2800 genes  
205 displayed at least 2-fold changes in the expression level of LCSA, MeJA, and MeJA+LCSA  
206 -treated leaves, respectively, relative to control leaves (Figure 2A). Of these, the number  
207 of differentially expressed genes (DEGs) of LCSA alone were greatly less than that in MeJA  
208 or MeJA+LCSA treatment group, in consistent with the inconspicuous phenotype between  
209 SA and control leaves (Figure 1). Therefore, our study is mainly concentrated on the  
210 differential expression of genes between MeJA and MeJA+LCSA.

211 To interpret the up-regulated and down-regulated DEGs resulting from the MeJA and  
212 MeJA+LCSA treatment, functional enrichment of Gene Ontology (GO) terms was  
213 performed using the hypergeometric test ( $P$ -value < 0.05). The analysis of biological  
214 process GO terms illustrated that most of the induced DEGs related to amino acid  
215 (Glutathione, Cyanamino acid, arginine, proline, alanine, aspartate and glutamate)  
216 metabolism, nitrogen metabolism, and flavonoid biosynthesis, whereas, the repressed  
217 DEGs mainly related to carbon metabolism, photosynthesis, and glycolysis (Figure 2B).  
218 These features of nitrogen and carbohydrate metabolism are consistent with the senescing  
219 phenotype of leaves. In contrast to MeJA alone, unexpectedly, LCSA together with MeJA  
220 treatment did not make much differences on the enriched biological processes (Figure 2C).  
221 The heatmap illustrated the top 50 up-regulated and down-regulated DEGs, which also  
222 revealed an extremely similar expression pattern between the DEGs of MeJA and  
223 MeJA+LCSA treatment (Figure 2D). These results indicated that LCSA does not appear to  
224 have dominant effects on the genetic regulatory network of basal metabolism like nitrogen  
225 metabolism, photosynthesis, and glycolysis.

## 226 **Network analysis identifies autophagy-related gene module**

227 Since the enrichment analysis only provided undifferentiated biological processes about  
228 basal metabolism, network analysis was conducted using DEGs that induced by MeJA and  
229 MeJA+LCSA, respectively. The protein-protein interactions (PPI) were collected from the  
230 STRING database, and only the PPIs with confidence scores higher than 0.7 were selected,  
231 resulting in a high confidence network with 719964 interactions and 17372 proteins.  
232 ClusterONE was used to identify functional protein modules, which were defined by the  
233 protein clusters including five or more than five members and having connection density  
234 over 0.5 (Cheng et al., 2019). According to such screening specifications, we identified 15  
235 gene modules in MeJA treatment group and 16 gene modules in MeJA+LCSA group,  
236 respectively (Figure S1 and S2). Of these, six gene modules were specially detected in the  
237 MeJA treatment group (Figure S3). Interestingly, MeJA together with SA exclusively

238 induced seven gene modules, covering genes involved in autophagy-related pathway,  
239 phytohormone response, ATP-binding cassette transporters, aquaporins, and flavonoid  
240 biosynthesis (Figure 3A). In this context, autophagy is an essential intracellular degradation  
241 system that plays important roles in nutrient remobilization during leaf senescence (Avila-  
242 Ospina et al., 2014). We found that the transcript abundance for ATG proteins (ATG4, ATG8,  
243 ATG9, and ATG12) was differentially sensitive to the MeJA+LCSA treatment. From the  
244 enriched biological processes and molecular functions, we observed that these ATGs are  
245 the core components that contribute to autophagosome mature and biogenesis (Figure 3B  
246 and 3C). Collectively, these results suggest a framework in which MeJA together with LCSA  
247 regulates the abundance of specific gene network, such as the autophagy process.

248 We next investigated whether the autophagy pathway was involved in LCSA-delayed  
249 leaf senescence. Ten ATG genes (ATG4A, ATG4B, ATG5, ATG6, ATG7, ATG8A, ATG8E,  
250 ATG8H, ATG12A, and ATG12B) that implemented in autophagosome formation were  
251 examined by RT-qPCR (Figure 4). In contrast to MeJA alone, most of these determined  
252 ATG genes, except for ATG8A and ATG8E, were up-regulated by the combined treatment  
253 group (MeJA+LCSA). The differential gene expression of ATG8 isoforms is possible due to  
254 they have different expression pattern in distinct tissues (Hanaoka et al., 2002).  
255 Interestingly, it should be mentioned that MeJA together with LCSA did not stimulate a  
256 much more increase in gene expression compared with control, especially LCSA treatment  
257 (Figure 4). These results indicate that restoration of ATG genes expression is closely  
258 related to LCSA-delayed leaf senescence.

### 259 **SA-delayed leaf senescence is dependent on a functional autophagy pathway**

260 To further resolve whether autophagy pathway was crucial for LCSA-delayed leaf  
261 senescence, two autophagy defective mutants (*atg5-1* and *atg7-2*), that involved in ATG8  
262 lipidation during phagophore elongation (Feng et al., 2014), were analyzed upon LCSA  
263 and/or MeJA treatment. In contrast to wild type (Col-0), leaves from *atg5-1* and *atg7-2*  
264 mutants were showed much more yellowing after incubated with MeJA for 5 days (Figure  
265 5A). As expect, the leaf yellowing phenotype was not alleviated when MeJA worked  
266 together with LCSA (Figure 5A). Consistently, the photochemical efficiency Fv/Fm in the  
267 *atg5-1* and *atg7-2* mutant leaves treated with MeJA+LCSA was not restored relative to that  
268 of the leaves treated with MeJA (Figure 5B). Similarly, none of the two mutants had  
269 recovered relative chlorophyll content as the Col-0 after combined treatment with MeJA  
270 and LCSA (Figure 5C). These genetic results clearly illustrated that the protection against  
271 MeJA-induced senescence by LCSA is dependent on a functional autophagy pathway.

## 272 **SA increases autophagy activity upon MeJA-induced leaf senescence**

273 Since autophagy pathway was verified involved in LCSA-delayed leaf senescence, we next  
274 further determined the detailed autophagy activity. Wild-type Arabidopsis plants expressing  
275 the eYFP-ATG8e fusion protein were subjected to LCSA and/or MeJA treatment, and the  
276 effects of LCSA on autophagy activity were analyzed by confocal microscopy of the YFP  
277 fluorescence. In control and LCSA treatment conditions, we observed a few fluorescent  
278 punctate structures that were identified previously as ATG8-tagged autophagosomes (or  
279 autophagic bodies) (Zhuang et al., 2013). Incubation of MeJA alone induced a slightly  
280 increase in accumulation of autophagic bodies (Figure 6A and 6B). However, when the  
281 detached leaves were subjected to combined treatment with MeJA and LCSA, there was  
282 a greatly increase in the fluorescent vesicles (Figure 6A and 6B). The statistical results  
283 showed that the number of autophagic bodies was more than 2-fold higher in MeJA+LCSA  
284 group than that of treatment with MeJA alone (Figure 6C and 6D). Taken together, our  
285 observations collectively suggest that LCSA activates the autophagy activity to delay  
286 MeJA-induced leaf senescence.

## 287 **DISCUSSION**

288 As the final stage of leaf development, leaf senescence is a complex process that involves  
289 thousands of genes and multiple layers of regulation. Mechanisms governing the specificity  
290 regulation of phytohormones and output gene expression are therefore of great interest.  
291 The primary objective of the work is to further explore the crosstalk between SA and JA  
292 signaling in regulating plant leaf senescence. We have concentrated on examining the  
293 mechanisms likely to underpin changes in the transcriptome in response to LCSA and/or  
294 MeJA. Specifically, an autophagy module was identified from the DEGs that exclusively  
295 induced by MeJA together with SA (Figure 3). Further results demonstrate that the  
296 upregulation of autophagy by LCSA serves important function in alleviating MeJA-induced  
297 leaf senescence (Figure 5 and 6).

298 Previously, we found that SA delays MeJA-induced leaf senescence in a concentration  
299 dependent manner (Ji et al, 2016). The dosage-dependent effect of SA also has been  
300 reported in plant root meristem regulation. SA at low levels (below 50  $\mu$ M) promotes  
301 adventitious roots and alters architecture of the root apical meristem, whereas high-  
302 concentration SA (>50  $\mu$ M) inhibits root growth (Pasternak et al., 2019). Such  
303 discrepancies are probably due to SA acts as a developmental regulator at low levels, but  
304 acts as a stress hormone at high levels (Pasternak et al., 2019). Interestingly, RNA-Seq

305 results showed that the number of DEGs in LCSA alone treatment were less than MeJA or  
306 LCSA and MeJA combined treatment group (Figure 2A), which consistent with LCSA itself  
307 did not have a discernible effect on senescence, showing the inconspicuous phenotype  
308 between LCSA and control leaves (Figure 1). Moreover, in contrast to MeJA alone, LCSA  
309 together with MeJA treatment did not make much differences on the biological process of  
310 GO terms (Figure 2C). These results indicated that LCSA at low level is more likely function  
311 as a signaling regulator, which does not have a marked impact on the basal metabolism at  
312 least at the genetic regulatory level.

313 Autophagy promotes cell survival by adapting cells to stress conditions both in plants  
314 and mammals. Recent reverse-genetic studies have revealed that autophagy is closely  
315 associated with plant senescence, and autophagy defective mutants like *atg2*, *atg5* and  
316 *atg7* all showed early yellowing leaf symptoms (Doelling et al., 2002; Yoshimoto et al.,  
317 2009). SA is one of the most promising phytohormones that contribute to the induction of  
318 autophagy under stress. It has previously been reported that autophagy negatively  
319 regulates cell death by controlling NPR1-dependent SA signaling during senescence in  
320 Arabidopsis (Yoshimoto et al., 2009). Here, the ClusterONE was applied to identify discrete  
321 gene modules based on PPI network. We identified several modules including autophagy-  
322 related network in DEGs that exclusively induced by MeJA together with LCSA (Figure 3A).  
323 Importantly, the protection against MeJA-induced senescence by LCSA was abolished in  
324 autophagy defective mutant *atg5-1* and *atg7-2* (Figure 5). These data strongly suggest an  
325 important role for autophagy in LCSA-alleviated leaf senescence. Notably, unlike the  
326 greatly increase of autophagic bodies induced by MeJA+LCSA, autophagosomes under  
327 LCSA alone treatment were not statistically significant when compared with control (Figure  
328 6). Nevertheless, it is worth pointing out that SA at 100  $\mu$ M, a high-concentration that could  
329 promote leaf senescence based on our previous study (Chai et al., 2016), greatly induced  
330 autophagic structures formation (Figure S4). In this context, we speculate that LCSA might  
331 be function like a priming regulator, which could initiate signal amplification and lead to a  
332 robust activation of stress response upon MeJA treatment. Actually, the priming induced  
333 by some plant activators (e.g.  $\beta$ -aminobutyric acid, and thiamine) are dependent on SA  
334 signaling (Ahn et al., 2005; Jung et al., 2009; Zhou et al., 2013). It would be interesting to  
335 test the priming effect of LCSA on leaf senescence in future research.

336 In summary, this study further investigated the interactions between SA and MeJA in  
337 plant senescence. Several modules including an autophagy-related (ATG) cluster were  
338 identified by analyzing the transcriptome data and protein interaction networks. Further

339 results showed that LCSA could upregulate autophagy to alleviate MeJA-induced leaf  
340 senescence. This was confirmed by founding that LCSA cannot alleviate the leaf yellowing  
341 phenotype in autophagy defective mutants upon MeJA treatment. Collectively, our work  
342 reveals LCSA tend to function as a signaling regulator to upregulate autophagy pathway,  
343 which serves as an important cellular mechanism responsible for alleviation of MeJA-  
344 induced leaf senescence.

#### 345 **Data availability**

346 RNA-seq data were deposited in the Sequence Read Archive (SRA) database  
347 <https://www.ncbi.nlm.nih.gov/sra> with accession no. PRJNA578602.

#### 348 **AUTHOR CONTRIBUTIONS**

349 JZ and LC designed the research. RY, JY, and YJ conducted the experiments. RY, XL, JL,  
350 JZ and LC analyzed data. JZ and LC wrote the manuscript. All authors read and approved  
351 the manuscript.

#### 352 **ACKNOWLEDGEMENTS**

353 Thanks for Professor Liwen Jiang (the Chinese University of Hong Kong) for giving the  
354 Arabidopsis seeds materials *atg5-1*, *atg7-2* and eYFP-ATG8e. Thanks for Yang Lv  
355 (Fengyuan biotechnology co. LTD, Shanghai, China) for the valuable suggestions for this  
356 manuscript. This work was supported by National Science Foundation of China (NSFC)  
357 (31600288); Guangdong Provincial Science and Technology Project (2016A020210127);  
358 SCNU Youth Teacher Research and Development Fund Project (671075); Scientific  
359 Research Projects of Guangzhou (201805010002).

#### 360 **CONFLICTS OF INTEREST**

361 The authors declare no conflict of interest.

## REFERENCES

- Anders, S., Huber, W. (2010). Differential expression analysis for sequence count data. *Genome Biol.* 11(10), R106. doi: 10.1186/gb-2010-11-10-r106
- Ahn, I. P., Kim, S., Lee, Y. H., Suh, S. C. (2007). Vitamin B1-induced priming is dependent on hydrogen peroxide and the NPR1 gene in Arabidopsis. *Plant Physiol.* 143(2), 838-848. doi: 10.1104/pp.106.092627
- Avila-Ospina, L., Moison, M., Yoshimoto, K., Masclaux-Daubresse, C. (2014). Autophagy, plant senescence, and nutrient recycling. *J. Exp. Bot.* 65(14), 3799-3811. doi: 10.1093/jxb/eru039
- Bhattacharjee, S. (2005). Reactive oxygen species and oxidative burst: roles in stress, senescence and signal transduction in plants. *Curr. Sci.* 89, 1113-1121.
- Chai, J., Liu, J., Zhou, J., Xing, D. (2014). Mitogen-activated protein kinase 6 regulates NPR1 gene expression and activation during leaf senescence induced by salicylic acid. *J. Exp. Bot.* 65(22), 6513-6528. doi: 10.1093/jxb/eru369
- Cheng, L., & Leung, K. S. (2018a). Identification and characterization of moonlighting long non-coding RNAs based on RNA and protein interactome. *Bioinformatics*, 34(20), 3519-3528. doi: 10.1093/bioinformatics/bty399
- Cheng, L., & Leung, K. S. (2018b). Quantification of non-coding RNA target localization diversity and its application in cancers. *J Mol. Cell Biol.* 10(2), 130-138. doi: 10.1093/jmcb/mjy006
- Cheng, L., Liu, P., Leung, K. S. (2017). SMILE: a novel procedure for subcellular module identification with localisation expansion. *IET Syst. Biol.* 12(2), 55-61. doi: 10.1049/iet-syb.2017.0085
- Cheng, L., Liu, P., Wang, D., Leung, K. S. (2019). Exploiting locational and topological overlap model to identify modules in protein interaction networks. *BMC bioinformatics*, 20(1), 23. doi: 10.1186/s12859-019-2598-7
- Cheng, L., Lo, L. Y., Tang, N. L., Wang, D., & Leung, K. S. (2016a). CrossNorm: a novel normalization strategy for microarray data in cancers. *Sci. Rep.* 6, 18898. doi: 10.1038/srep18898
- Cheng, L., Wang, X., Wong, P. K., Lee, K. Y., Li, L., Xu, B., et al. (2016b). ICN: a normalization method for gene expression data considering the over-expression of informative genes. *Mol. BioSyst.* 12(10), 3057-3066. doi: 10.1039/c6mb00386a
- Coombs, J., G. Hind, R. C. Leegood, L. L. Tieszen and A. Vonshak (1987). Analytical Techniques. In: *Techniques in Bioproductivity and photosynthesis 2nd Edition.* (Eds) J. Coombs, D. O. Hall, S. P. Long and J. M. O. Scurlock. 219-220. Pergamon Press.
- Doelling, J. H., Walker, J. M., Friedman, E. M., Thompson, A. R., Vierstra, R. D. (2002). The APG8/12-activating enzyme APG7 is required for proper nutrient recycling and senescence in Arabidopsis thaliana. *J. Biol. Chem.* 277(36), 33105-33114.
- Feng, Y., He, D., Yao, Z., & Klionsky, D. J. (2014). The machinery of macroautophagy. *Cell Res.* 24(1), 24-41. doi: 10.1038/cr.2013.168
- Gan S, Amasino RM. 1995. Inhibition of leaf senescence by autoregulated production of cytokinin. *Science* 270:1986-1988. doi: 10.1126/science.270.5244.1986
- Ji, Y., Liu, J., Xing, D. (2016). Low concentrations of salicylic acid delay methyl jasmonate-induced leaf senescence by up-regulating nitric oxide synthase activity. *J.*

- Exp. Bot. 67(17), 5233-5245. doi: 10.1093/jxb/erw280
- Jung, H. W., Tschaplinski, T. J., Wang, L., Glazebrook, J., Greenberg, J. T. (2009). Priming in systemic plant immunity. *Science*, 324(5923), 89-91. doi: 10.1126/science.1170025
- Hanaoka, H., Noda, T., Shirano, Y., Kato, T., Hayashi, H., Shibata, D., et al. (2002). Leaf senescence and starvation-induced chlorosis are accelerated by the disruption of an *Arabidopsis* autophagy gene. *Plant Physiol.* 129(3), 1181-1193. doi: 10.1104/pp.011024
- He, Y., Fukushige, H., Hildebrand, D.F., Gan, S. 2002. Evidence supporting a role of jasmonic acid in *Arabidopsis* leaf senescence. *Plant Physiol.* 128(3), 876-884. doi: 10.1104/pp.010843
- Hung, K.T., Kao, C.H. 2004. Hydrogen peroxide is necessary for abscisic acid-induced senescence of rice leaves. *J. Plant Physiol.* 161(12), 1347-1357. doi: 10.1016/j.jplph.2004.05.011
- Li, F., Chung, T., Vierstra, R. D. (2014). AUTOPHAGY-RELATED11 plays a critical role in general autophagy-and senescence-induced mitophagy in *Arabidopsis*. *Plant Cell* 26(2), 788-807. doi: 10.1105/tpc.113.120014
- Love, M. I., Huber, W., Anders, S. (2014). Moderated estimation of fold change and dispersion for RNA-seq data with DESeq2. *Genome Biol.* 15(12), 550. doi: 10.1186/s13059-014-0550-8
- Lim, P.O., Woo, H.R., & Nam, H.G. (2003). Molecular genetics of leaf senescence in *Arabidopsis*. *Trends Plant Sci.* 8(6), 272-278. doi: 10.1016/S1360-1385(03)00103-1
- Lim, P.O., Kim, H.J., Nam, H.G. 2007. Leaf senescence. *Annu. Rev. Plant Biol.* 58, 115-136. doi: 10.1146/annurev.arplant.57.032905.105316
- Masclaux, C., Valadier, M.H., Brugiére, N., Morot-Gaudry, J.F., Hirel, B. 2000. Characterization of the sink/source transition in tobacco (*Nicotiana tabacum* L.) shoots in relation to nitrogen management and leaf senescence. *Planta* 211, 510-518. doi: 10.1007/s004250000310
- Miao Y., Zentgraf U. 2007. The antagonist function of *Arabidopsis* WRKY53 and ESR/ESP in leaf senescence is modulated by the jasmonic and salicylic acid equilibrium. *Plant Cell* 19, 819-830. doi: 10.1105/tpc.106.042705
- Morris, K., Mackerness, S.A., Page, T., John, C.F., Murphy, A.M., et al. 2000. Salicylic acid has a role in regulating gene expression during senescence. *Plant J.* 23:677-685. doi: 10.1046/j.1365-313x.2000.00836.x
- Pasternak, T., Groot, E. P., Kazantsev, F. V., Teale, W., Omelyanchuk, N., Kovrizhnykh, V., et al. (2019). Salicylic acid affects root meristem patterning via auxin distribution in a concentration-dependent manner. *Plant Physiol.* 180(3), 1725-1739. doi: 10.1104/pp.19.00130
- Quirino, B.F., Noh, Y.S., Himelblau, E., Amasino, R.M. (2000). Molecular aspects of leaf senescence. *Trends Plant Sci.* 5(7), 278-282. doi: 10.1016/S1360-1385(00)01655-1
- Schippers, J.H. (2015). Transcriptional networks in leaf senescence. *Curr. Opin. Plant Biol.* 27, 77-83. doi: 10.1016/j.pbi.2015.06.018
- Szklarczyk, D., Franceschini, A., Wyder, S., Forslund, K., Heller, D., Huerta-Cepas, J., et al. (2014). STRING v10: protein–protein interaction networks, integrated over the

- tree of life. *Nucleic Acids Res.* 43(1), 447-452. doi: 10.1093/nar/gku1003
- Thaler, J. S., Humphrey, P. T., & Whiteman, N. K. (2012). Evolution of jasmonate and salicylate signal crosstalk. *Trends Plant Sci.* 17(5), 260-270. doi: 10.1016/j.tplants.2012.02.010
- van der Graaff, E., Schwacke, R., Schneider, A., Desimone, M., Flugge, U.I., Kunze, R. 2006. Transcription analysis of Arabidopsis membrane transporters and hormone pathways during developmental and induced leaf senescence. *Plant Physiol.* 141:776-792. doi: 10.1104/pp.106.079293
- Xiong, Y., Contento, A. L., Bassham, D. C. (2005). AtATG18a is required for the formation of autophagosomes during nutrient stress and senescence in Arabidopsis thaliana. *Plant J.* 42(4), 535-546. doi: 10.1111/j.1365-313X.2005.02397.x
- Xiong, Y., Contento, A. L., Nguyen, P. Q., Bassham, D. C. (2007). Degradation of oxidized proteins by autophagy during oxidative stress in Arabidopsis. *Plant Physiol.* 143(1), 291-299. doi: 10.1104/pp.106.092106
- Yoshida, S. (2003). Molecular regulation of leaf senescence. *Curr. Opin. Plant Biol.* 6(1), 79-84. doi: 10.1016/S1369526602000092
- Yoshimoto, K., Jikumaru, Y., Kamiya, Y., Kusano, M., Consonni, C., Panstruga, R., et al. (2009). Autophagy negatively regulates cell death by controlling NPR1-dependent salicylic acid signaling during senescence and the innate immune response in Arabidopsis. *Plant Cell*, 21(9), 2914-2927. doi: 10.1105/tpc.109.068635
- Yue, H., Nie, S., Xing, D. (2012). Over-expression of Arabidopsis Bax inhibitor-1 delays methyl jasmonate-induced leaf senescence by suppressing the activation of MAP kinase 6. *J. Exp. Bot.* 63(12), 4463-4474. doi: 10.1093/jxb/ers122
- Zeng, L., Wang, Y., Zhou, J. (2016). Spectral analysis on origination of the bands at 437 nm and 475.5 nm of chlorophyll fluorescence excitation spectrum in Arabidopsis chloroplasts. *Luminescence*, 31(3), 769-774. doi: 10.1002/bio.3022
- Zhou, J., Sun, A., Xing, D. (2013). Modulation of cellular redox status by thiamine-activated NADPH oxidase confers Arabidopsis resistance to *Sclerotinia sclerotiorum*. *J. Exp. Bot.* 64(11), 3261-3272. doi: 10.1093/jxb/ert166
- Zhou, J., Zeng, L., Liu, J., Xing, D. (2015). Manipulation of the xanthophyll cycle increases plant susceptibility to *Sclerotinia sclerotiorum*. *PLoS Pathog.* 11(5), e1004878. doi: 10.1371/journal.ppat.1004878
- Zhuang, X., Wang, H., Lam, S. K., Gao, C., Wang, X., Cai, Y., Jiang, L. (2013). A BAR-domain protein SH3P2, which binds to phosphatidylinositol 3-phosphate and ATG8, regulates autophagosome formation in Arabidopsis. *Plant Cell*, 25(11), 4596-4615. doi: 10.1105/tpc.113.118307

362 **FIGURE LEGENDS**

363 **Figure 1. LCSA alleviates MeJA-induced leaf senescence.** (A) Phenotypes of detached  
364 leaves under LCSA and/or MeJA treatments. The 3rd and 4th rosette leaves were  
365 incubated in 3 mM MES buffer (pH 5.8) containing LCSA (10  $\mu$ M) or MeJA (50  $\mu$ M) alone  
366 or in combination (MeJA+LCSA) under continuous light for 5 d. (B and C) Measurement of  
367 the maximum quantum efficiency of photosystem II (PSII) photochemistry (Fv/Fm) (B) and  
368 total chlorophyll content (C) after LCSA and/or MeJA treatments. The percentages of  
369 Fv/Fm and chlorophyll content are relative to the initial levels at time zero. Data were the  
370 mean  $\pm$  SE of three independent experiments. Different letters indicate statistically  
371 significant differences between each treatment (Duncan's multiple range test,  $p < 0.05$ ).

372 **Figure 2. RNA-Seq analyses of differentially expressed genes (DEGs) in samples**  
373 **treated with LCSA, MeJA and LCSA+MeJA.** (A) Venn diagram showing the overlap of  
374 DEGs between LCSA, MeJA and LCSA+MeJA-treated samples. (B and C) The pathway  
375 enrichment analysis of up or down -regulated DEGs induced by MeJA alone (B) or  
376 LCSA+MeJA (C). (D) The heatmap showing expression of top 50 up-regulated and down-  
377 regulated DEGs between MeJA and MeJA+LCSA treatment group.

378 **Figure 3. Network analysis identifies distinct signal modules in the DEGs exclusively**  
379 **induced by LCSA+MeJA treatment.** (A) Interconnected clusters enriched among the 889  
380 genes and their interactions with neighboring genes. The autophagy specific module was  
381 drawn in a red dotted line. Genes are colored in red if they are induced and in blue if they  
382 are repressed. (B and C) Biological process (B) and molecular function (C) classification  
383 in gene ontology analysis of the DEGs that identified in coexpression networks.

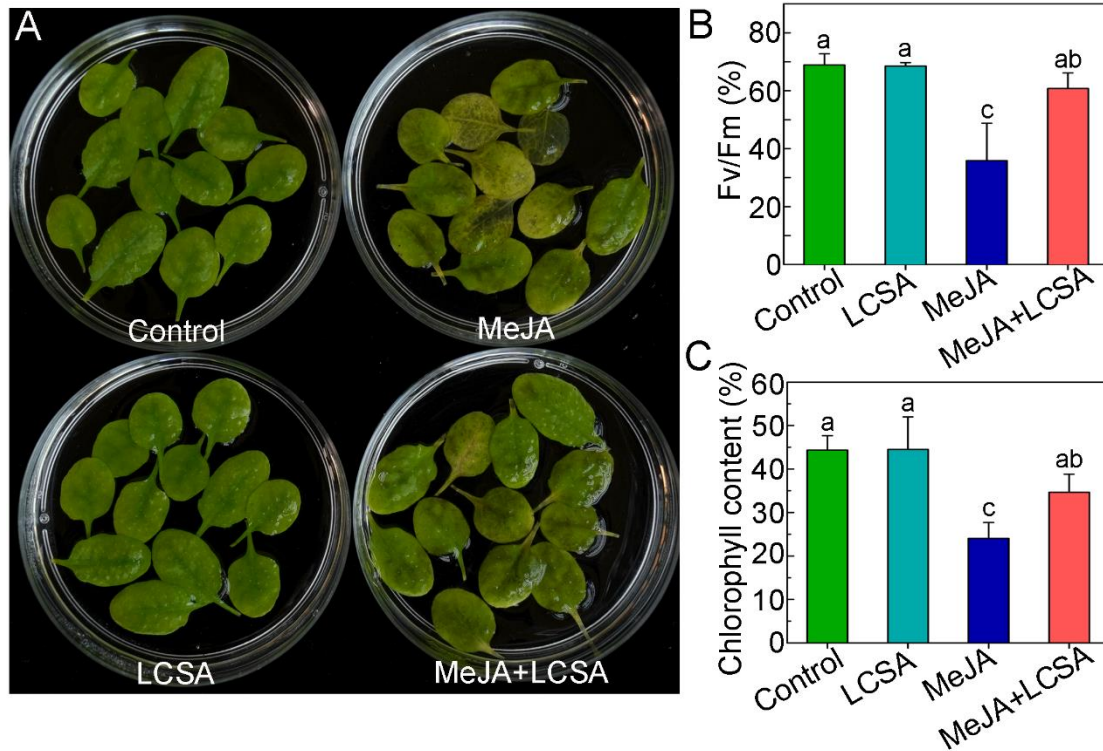
384 **Figure 4. RT-qPCR confirmation of differentially expressed genes that involved in**  
385 **regulation of autophagy.** The relative mRNA expression levels were calculated using the  
386  $\Delta\Delta$ Ct method. The value of each ATG genes were relative to the initial levels at time zero  
387 of treatment. Data were the mean  $\pm$  SE of three independent experiments. Different letters  
388 in each genes indicate statistically significant differences between the treatments  
389 (Duncan's multiple range test,  $p < 0.05$ ).

390 **Figure 5. Defective in autophagy restrains the effect of SA on the senescence**  
391 **symptoms.** (A) Phenotypes of LCSA-alleviated senescence in Col-0 and autophagy  
392 defective mutants (*atg5-1* and *atg7-2*). Detached leaves from four-week-old Col-0, *atg5-1*,  
393 and *atg7-2* plants were transferred to MES buffer (pH 5.8) containing LCSA (10  $\mu$ M) or  
394 MeJA (50  $\mu$ M) or both MeJA and LCSA under continuous light and photographs were taken  
395 after 5 days of treatment. (B and C) Relative Fv/Fm (B) chlorophyll levels (C) in the leaves  
396 of the Col-0, *atg5-1*, and *atg7-2* described in (A). Data were the mean  $\pm$  SE of three  
397 independent experiments. Different letters indicate statistically significant differences  
398 between the treatments (Duncan's multiple range test,  $p < 0.05$ ).

399 **Figure 6. LCSA enhances the formation of autophagosomes upon MeJA-induced**  
400 **leaf senescence.** (A) Microscopic analyses of autophagosome-related structures in the  
401 mesophyll cells of eYFP-ATG8e plant under LCSA or MeJA or both MeJA and LCSA  
402 treatment. (B) Examination of autophagic bodies accumulated in the vacuoles. Conca,

403 concanamycin A. Bars, 20  $\mu\text{m}$ . (C and D) Statistical analysis of the puncta numbers  
404 displayed in (A) and (B), respectively. The number of puncta was calculated per 0.01  $\text{mm}^2$   
405 from at least 15 pictures. This experiment was repeated in triplicate with similar results.  
406 Different letters indicate statistically significant differences between the treatments  
407 (Duncan's multiple range test,  $p < 0.05$ ).

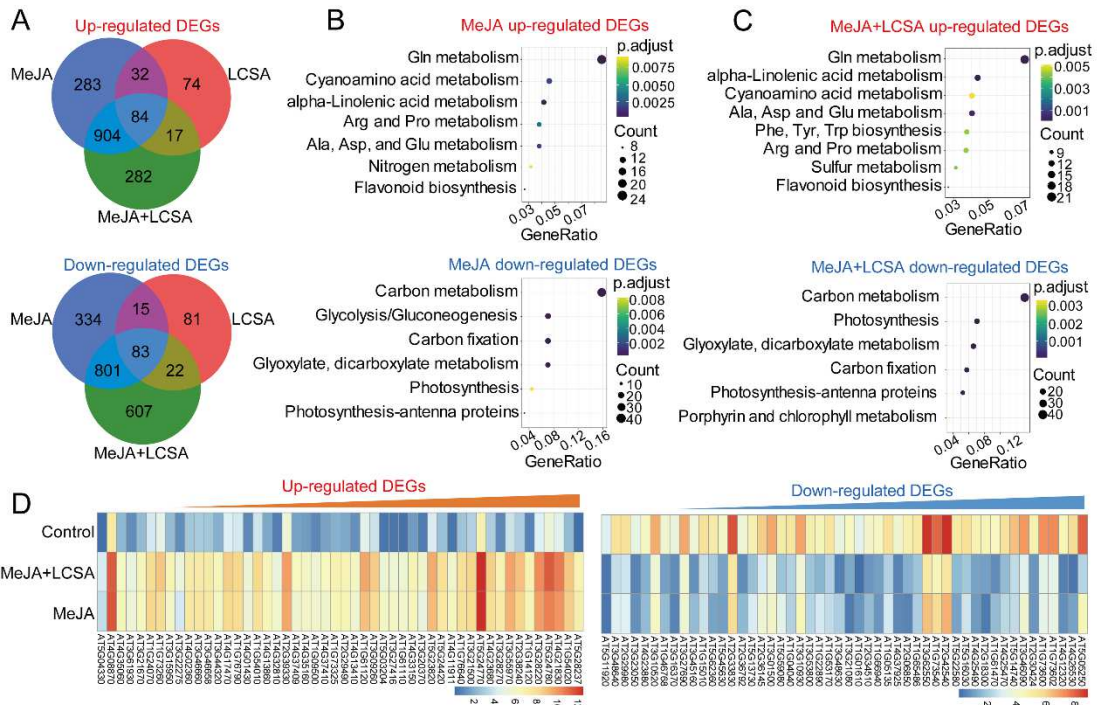
408



409

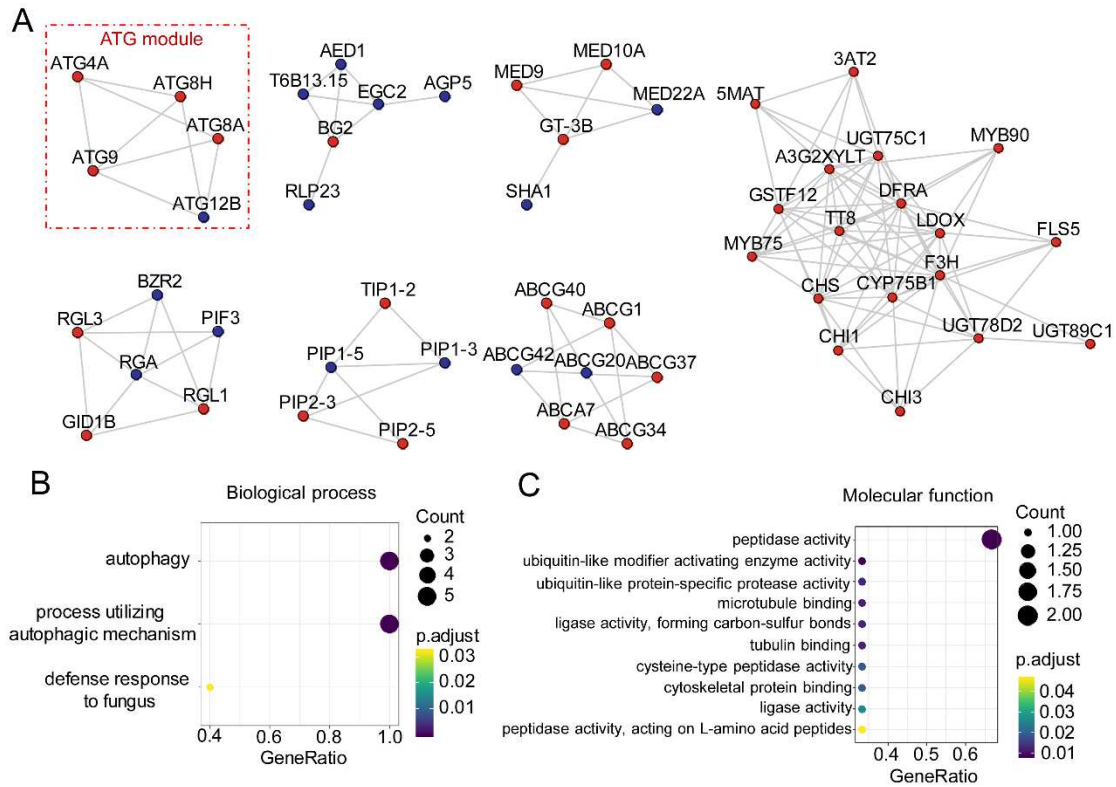
410 **Figure 1. LCSA alleviates MeJA-induced leaf senescence.** (A) Phenotypes of detached  
 411 leaves under LCSA and/or MeJA treatments. The 3rd and 4th rosette leaves were  
 412 incubated in 3 mM MES buffer (pH 5.8) containing LCSA (10  $\mu$ M) or MeJA (50  $\mu$ M) alone  
 413 or in combination (MeJA+LCSA) under continuous light for 5 d. (B and C) Measurement of  
 414 the maximum quantum efficiency of photosystem II (PSII) photochemistry (Fv/Fm) (B) and  
 415 total chlorophyll content (C) after LCSA and/or MeJA treatments. The percentages of  
 416 Fv/Fm and chlorophyll content are relative to the initial levels at time zero. Data were the  
 417 mean  $\pm$  SE of three independent experiments. Different letters indicate statistically  
 418 significant differences between each treatment (Duncan's multiple range test,  $p < 0.05$ ).

419



420  
 421  
 422  
 423  
 424  
 425  
 426  
 427

**Figure 2. RNA-Seq analyses of differentially expressed genes (DEGs) in samples treated with LCSA, MeJA and LCSA+MeJA.** (A) Venn diagram showing the overlap of DEGs between LCSA, MeJA and LCSA+MeJA-treated samples. (B and C) The pathway enrichment analysis of up or down -regulated DEGs induced by MeJA alone (B) or LCSA+MeJA (C). (D) The heatmap showing expression of top 50 up-regulated and down-regulated DEGs between MeJA and MeJA+LCSA treatment group.



428

429

**Figure 3. Network analysis identifies distinct signal modules in the DEGs**

430

**exclusively induced by LCSA+MeJA treatment.** (A) Interconnected clusters enriched

431

among the 889 genes and their interactions with neighboring genes. The autophagy

432

specific module was drawn in a red dotted line. Genes are colored in red if they are

433

induced and in blue if they are repressed. (B and C) Biological process (B) and molecular

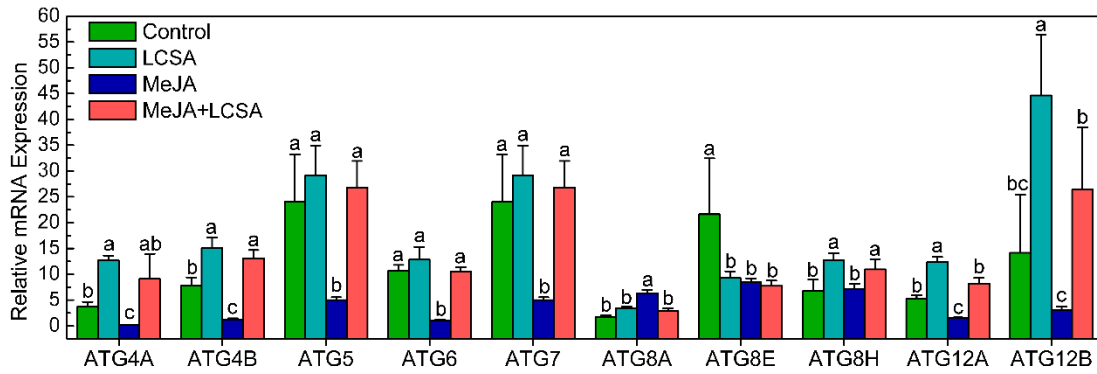
434

function (C) classification in gene ontology analysis of the DEGs that identified in

435

coexpression networks.

436



437

438

439

440

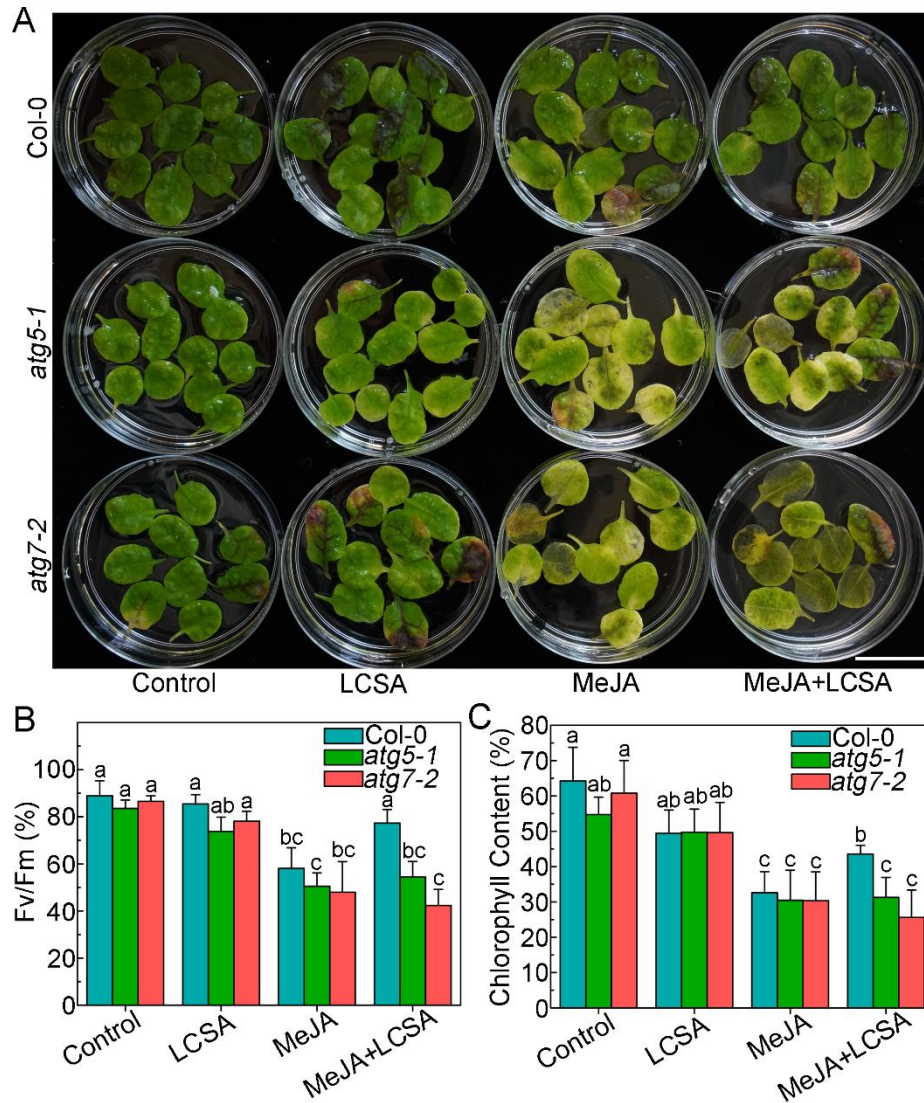
441

442

443

444

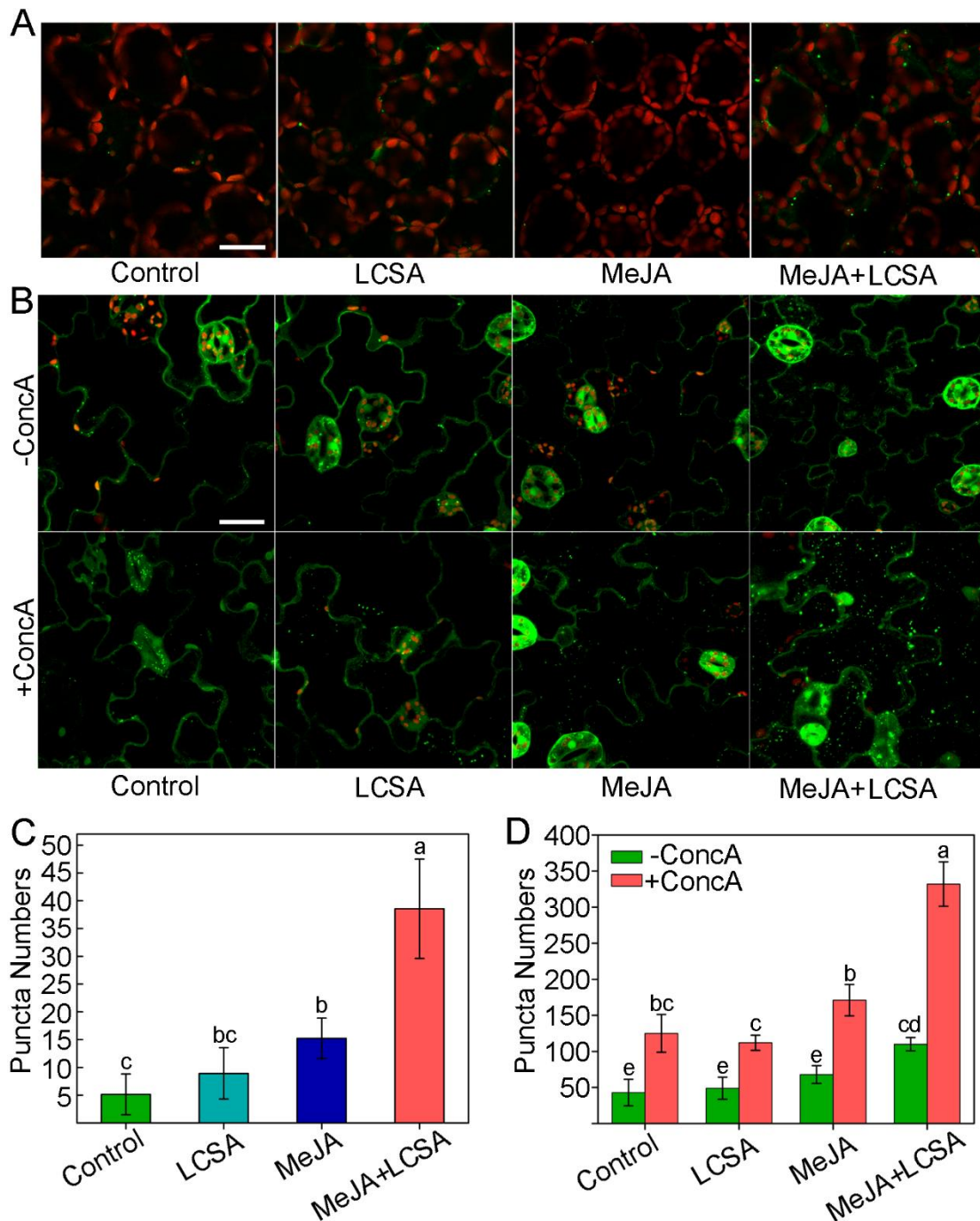
**Figure 4. RT-qPCR confirmation of differentially expressed genes that involved in regulation of autophagy.** The relative mRNA expression levels were calculated using the  $\Delta\Delta C_t$  method. The value of each ATG genes were relative to the initial levels at time zero of treatment. Data were the mean  $\pm$  SE of three independent experiments. Different letters in each genes indicate statistically significant differences between the treatments (Duncan's multiple range test,  $p < 0.05$ ).



445

446 **Figure 5. Defective in autophagy restrains the effect of SA on the senescence**  
 447 **symptoms.** (A) Phenotypes of LCSA-alleviated senescence in Col-0 and autophagy  
 448 defective mutants (*atg5-1* and *atg7-2*). Detached leaves from four-week-old Col-0, *atg5-1*,  
 449 and *atg7-2* plants were transferred to MES buffer (pH 5.8) containing LCSA (10  $\mu$ M) or  
 450 MeJA (50  $\mu$ M) or both MeJA and LCSA under continuous light and photographs were taken  
 451 after 5 days of treatment. (B and C) Relative Fv/Fm (B) chlorophyll levels (C) in the leaves  
 452 of the Col-0, *atg5-1*, and *atg7-2* described in (A). Data were the mean  $\pm$  SE of three  
 453 independent experiments. Different letters indicate statistically significant differences  
 454 between the treatments (Duncan's multiple range test,  $p < 0.05$ ).

455



456

457 **Figure 6. LCSA enhances the formation of autophagosomes upon MeJA-induced**  
 458 **leaf senescence.** (A) Microscopic analyses of autophagosome-related structures in the  
 459 mesophyll cells of eYFP-ATG8e plant under LCSA or MeJA or both MeJA and LCSA  
 460 treatment. (B) Examination of autophagic bodies accumulated in the vacuoles. ConcA,  
 461 concanamycin A. Bars, 20  $\mu$ m. (C and D) Statistical analysis of the puncta numbers  
 462 displayed in (A) and (B), respectively. The number of puncta was calculated per 0.01 mm<sup>2</sup>  
 463 from at least 15 pictures. This experiment was repeated in triplicate with similar results.  
 464 Different letters indicate statistically significant differences between the treatments  
 465 (Duncan's multiple range test,  $p < 0.05$ ).

466

## Supplementary Files

This is a list of supplementary files associated with this preprint. Click to download.

- [SupplementaryMaterials.pdf](#)